TOPICAL REVIEW — Magnetism, magnetic materials, and interdisciplinary research

Formation of multifunctional Fe_3O_4/Au composite nanoparticles for dual-mode MR/CT imaging applications*

Hu Yong(胡 勇), Li Jing-Chao(李静超), Shen Ming-Wu(沈明武)†, and Shi Xiang-Yang(史向阳)‡

College of Chemistry, Chemical Engineering and Biotechnology, Donghua University, Shanghai 201620, *China*

(Received 1 May 2014; revised manuscript received 26 May 2014; published online 5 June 2014)

Recent advances with iron oxide/gold (Fe_3O_4/Au) composite nanoparticles (CNPs) in dual-modality magnetic resonance (MR) and computed tomography (CT) imaging applications are reviewed. The synthesis and assembly of "dumbbell-like" and "core/shell" Fe_3O_4/Au CNPs is introduced. Potential applications of some developed Fe_3O_4/Au CNPs as contrast agents for dual-mode MR/CT imaging applications are described in detail.

Keywords: iron oxide nanoparticles, gold nanoparticles, magnetic resonance imaging, computed tomography imaging

PACS: 87.57.Q−, 87.61.−c, 75.50.−y, 87.85.Rs **DOI:** 10.1088/1674-1056/23/7/078704

1. Introduction

Molecular imaging is considered to be a powerful technology for disease diagnosis. Due to the fact that each imaging modality displays its inherent limits and drawbacks,[1] it is essential to perform dual- or multi-mode imaging for accurate disease detection. In this context, development of multifunctional nanoparticulate systems that are able to integrate two or more imaging contrast agents within one particulate system is necessary. Recent advances in nanotechnology have enabled the generation of various nanoparticle (NP) systems for dual-modality imaging applications, such as T_1- and T_2-weighted MR imaging,[2–5] MR/CT imaging,[1,6–8] ultrasonic/MR imaging,[9,10] MR/PET imaging,[11–13] MR/fluorescence imaging,[14–16] and MR/optical imaging.[17–20]

Among these different dual-mode combinations for molecular imaging, MR/CT imaging has attracted widespread attention. MR imaging is a powerful and non-invasive technique with high spatial resolution, tomographic capabilities, and a non-ionizing type of radiation. Meanwhile, CT imaging technology is also recognized as another reliable molecular imaging mode because its spatial and density resolution are greater than those of other imaging modes. Therefore, the combination of MR and CT imaging is of great clinical significance.

For MR imaging applications, superparamagnetic iron oxide (Fe_3O_4) NPs have been widely used as negative contrast agents in recent decades due to their ability to affect the MR signal by dephasing transverse magnetization and reducing the T_2 value of water protons.[21–23] Recently, some Fe_3O_4-based multifunctional composite NPs (CNPs) have been explored for multi-modal imaging applications through integration with other imaging elements, such as Gd complexes, Ag NPs, Au NPs/rods, Cu compounds, etc.[2,6,24,25] On the other hand, gold (Au) NPs have been widely applied in many different fields,[26–29] especially as a kind of novel contrast agent for CT imaging, because of their higher X-ray absorption coefficient and good biocompatibility after appropriate surface modification.[30–34] Therefore, synthesis of Fe_3O_4/Au CNPs for MR/CT dual-mode imaging has received a surge of interest. Likewise, the versatility of nanotechnology has enabled the preparation of Fe_3O_4/Au "core/shell" CNPs via direct deposition of Au NPs onto the surface of Fe_3O_4 NPs,[35,36] enabled the formation of Fe_3O_4/Au "core/shell" CNPs by a sonochemical method,[37] and enabled the creation of Fe_3O_4/Au CNPs via decomposition of $Fe(CO)_5$ on the surface of the Au NPs, followed by oxidation.[38–40] Some of these Fe_3O_4/Au CNPs have been used for dual-modality MR/CT imaging applications.

This review mainly reports recent advances in the synthesis of Fe_3O_4/Au CNPs and the applications of these CNPs for MR/CT dual-mode imaging. This review will not cover all aspects of the Fe_3O_4/Au CNPs. Rather, it will introduce some key developments in the synthesis of several kinds of Fe_3O_4/Au CNPs for MR/CT imaging applications. This review starts from a brief introduction, and then discusses different approaches to preparing Fe_3O_4/Au CNPs with different structures and the uses of these CNPs for dual-mode MR/CT imaging applications. The paper ends with a brief conclusion and a future perspective discussion.

*Project supported by the National Natural Science Foundation of China (Grant Nos. 81351050, 81101150, and 21273032), the Fund of the Science and Technology Commission of Shanghai Municipality, China (Grant Nos. 11nm0506400 and 12520705500), and the Program for Professor of Special Appointment (Eastern Scholar) at Shanghai Institutions of Higher Learning, China.

†Corresponding author. E-mail: mwshen@dhu.edu.cn

‡Corresponding author. E-mail: xshi@dhu.edu.cn

© 2014 Chinese Physical Society and IOP Publishing Ltd

2. Synthesis or formation of Fe_3O_4/Au CNPs

Fe_3O_4/Au CNPs can be categorized into "dumbbell-like" vs "core/shell" structures. In this part, we will introduce the synthesis or formation of both.

2.1. "Dumbbell-like" structured CNPs

The "dumbbell-like" structured Fe_3O_4/Au CNPs have generally been synthesized by one of two strategies. In the first, iron pentacarbonyl is decomposed on the surfaces of Au NPs in the presence of oleic acid and oleylamine (Fig. 1), followed by subsequent functionalization via a surfactant exchange process.[40] The CNPs so formed possess a unique structure: one Fe_3O_4 NP is linked to one Au NP (Fig. 2).[38] These CNPs can be further modified through different techniques for various applications. In the second strategy, iron-oleate and gold-oleylamine are mixed in oleylamine and 1-octadecene, followed by thermal decomposition of these precursors to yield the unique "dumbbell-like" CNPs.[41,42] The CNPs so formed may display interesting catalytic, magnetic, and optical properties.[43,44] Fe_3O_4/Au "dumbbell-like" CNPs have been proven to be biocompatible in a certain concentration range and may be used for magnetic and optical applications in biomedicine.[45,46]

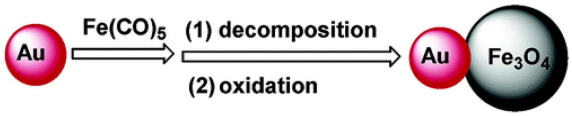


Fig. 1. Schematic illustration of the preparation of "dumbbell-like" Fe_3O_4/Au CNPs.[40]

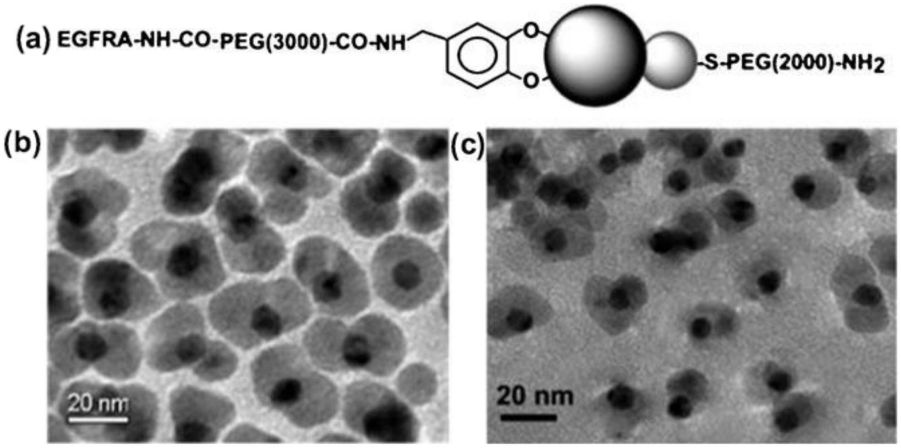


Fig. 2. (a) Schematic illustration of surface functionalization of the Fe_3O_4/Au CNPs. TEM images of the 8–20 nm Fe_3O_4/Au CNPs before (b) and after (c) surface modification.[38]

2.2. "Core/shell" structured CNPs

Besides the formation of Fe_3O_4/Au "dumbbell-like" CNPs, "core/shell" type Fe_3O_4/Au CNPs have also been formed via a simple assembly process. In a recent effort, Bao *et al.*[47] fabricated biofunctional "core/shell" Fe_3O_4/Au CNPs by simply linking two separately prepared NPs via chemical bonds (Fig. 3). Compared to the Fe_3O_4 NPs (4–20 nm) used for formation of "dumbbell-like" Fe_3O_4/Au CNPs,[38] the particles they used in this study were much larger. Furthermore, the Fe_3O_4/Au CNPs can be easily modified with other functional molecules to realize various bio-applications. Unfortunately, this type of larger CNPs is prone to precipitate and lacks sufficient colloidal stability, which may not be suitable for *in vivo* biomedical applications.

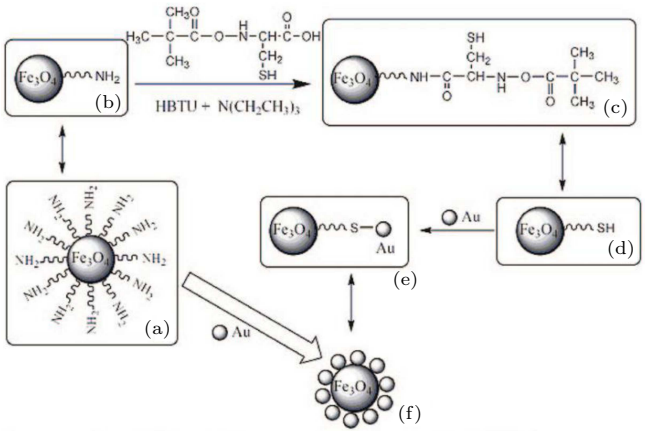


Fig. 3. Schematic illustration of bifunctional Fe_3O_4/Au CNP synthesis. Amino-functionalized Fe_3O_4 NPs (a, simplified as b for the convenience of illustration) were first modified by Boc-L-cysteine to have surface thiol groups (c, simplified as d). Gold NPs were then conjugated onto the surface of Fe_3O_4 NPs to form the expected bifunctional Fe_3O_4/Au CNPs (f, simplified as e).[47]

To improve the colloidal stability of the Fe_3O_4/Au CNPs, it is essential to select smaller sized Fe_3O_4 NPs as core particles for the formation of "core/shell" structured Fe_3O_4/Au CNPs. In a recent study, Caruntu *et al.* reported the successful attachment of 2–3 nm Au NPs onto the surface of Fe_3O_4 core NPs (10 nm) through a simple "two-step" chemically controlled procedure.[48] In this approach, Fe_3O_4 NPs were synthesized from a stable colloidal methanolic solution, followed

by coating with amino-terminated silane to render the particles with positive charges. Then, the Fe_3O_4 NPs were treated with a colloidal solution of negatively charged Au NPs (Fig. 4). The transmission electron microscope (TEM) results clearly indicate the successful formation of Fe_3O_4/Au CNPs (Fig. 5). The colloidal Fe_3O_4/Au CNPs were highly stable against separation and exhibited magnetic properties similar to those of the parent Fe_3O_4 nanocrystals, suggesting that the coating of Au NPs does not appreciably compromise the magnetic properties of the Fe_3O_4 core particles.

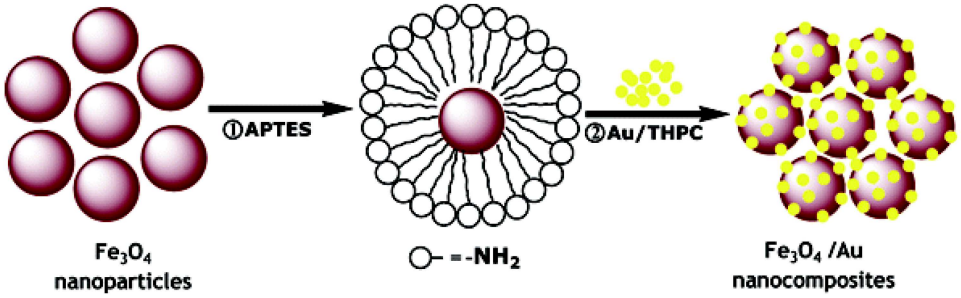


Fig. 4. Schematic illustration of bifunctional Fe_3O_4/Au CNP synthesis.[48]

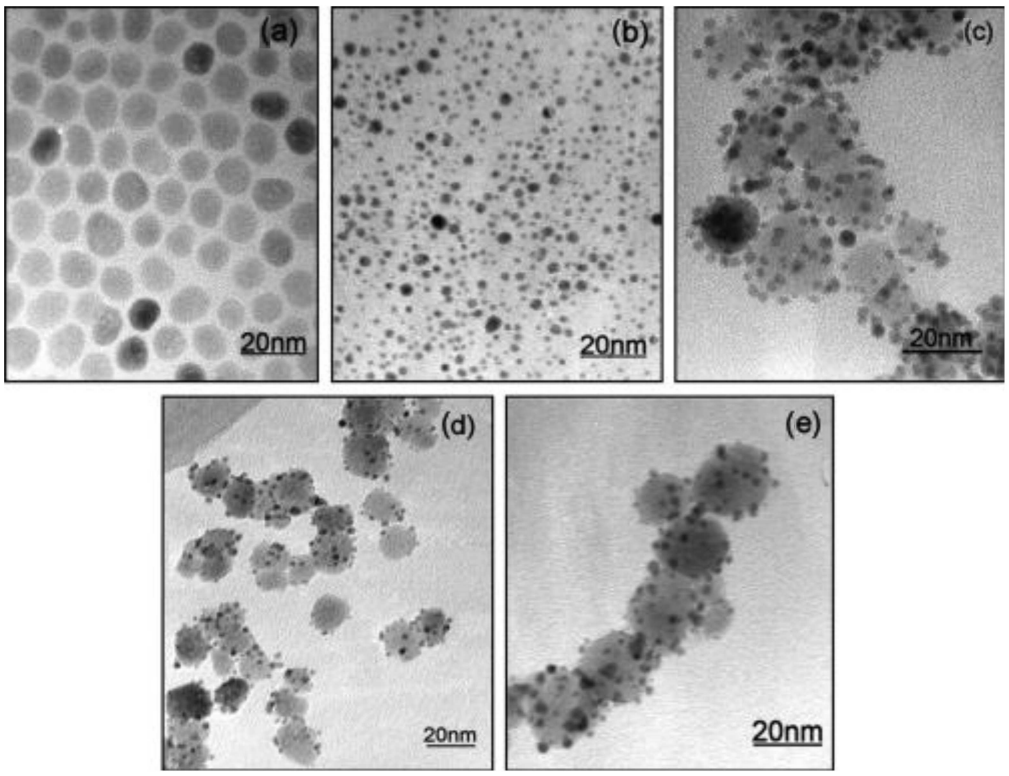


Fig. 5. Typical TEM images of the as-prepared Fe_3O_4 NPs obtained from a mixture of DEG and NMDEA (3:1, *w*/*w*) (a), the colloidal Au particles (b), the freshly prepared Fe_3O_4/Au CNPs (c), and the Fe_3O_4/Au CNPs aged for 2 (d) and 5 months (e), and sonicated for 60 min.[48]

Another "two-step" protocol for direct coating of Au onto the Fe_3O_4 core NPs was reported by Carril *et al.*[49] In brief, Fe_3O_4 NPs (3.2 nm) were obtained by thermal decomposition of $Fe(acac)_3$ in the presence of oleic acid and oleylamine at a high temperature. Under similar conditions, the obtained Fe_3O_4 NPs were further covered with a gold layer by thermal decomposition of gold (III) acetate and protected by a coating of oleic acid to afford the formation of Fe_3O_4/Au CNPs with a size of 6.1 nm. The NPs underwent a ligand exchange step with a 1:1 mixture of carboxy-terminal ligand and glucose-terminal ligand to yield water-soluble Fe_3O_4@Au NPs.

To generate "core/shell" Fe_3O_4/Au CNPs, seed-mediated growth methods have also been developed.[50–52] In this process, preformed Ag- or Au-decorated Fe_3O_4 hybrid NPs are used as seeds, and Fe_3O_4/Au CNPs with a core/shell structure can be formed by dropping the seeds into the gold growth solution. For instance, Hu *et al.*[50] first prepared Fe_3O_4@polyphosphazene@Au seeds with the help of $NaBH_4$, and then exposed the seed particles to chloroauric acid ($HAuCl_4$) solution to form Au shell on the surface

of the seeds via sodium citrate reduction at 100 °C. In another work,[51] Ag-decorated Fe_3O_4 NPs were injected into the growth solution of $HAuCl_4$, cetyltrimethylammonium bromide (CTAB), and silver nitrate ($AgNO_3$) for subsequent formation of pin-like "core/shell" Fe_3O_4/Au CNPs using ascorbic acid as a reducing agent. The added Ag ions play an important role in the Au shell growth process because they can block the crystal growth in some direction, similar to the formation of star-shaped "core/shell" Fe_3O_4/Au CNPs reported in the literature.[52]

Beyond the above-mentioned approach to synthesizing Fe_3O_4/Au CNPs, a polymer-mediated self-assembly approach can also be used to generate Fe_3O_4/Au CNPs with good water dispersibility, colloidal stability, and biocompatibility.[21,23,53–55] In a recent report, Cai *et al.*[6] developed a convenient approach to assembling dendrimer-entrapped Au NPs (Au DENPs) onto Fe_3O_4 core NPs through a layer-by-layer (LbL) self-assembly technique and dendrimer chemistry. In this work, positively charged Fe_3O_4 NPs were first prepared by a controlled co-precipitation approach, and then were used as core particles for subsequent electrostatic LbL assembly of poly(γ-glutamic acid) (PGA) and poly(L-lysine) (PLL) to form PGA/PLL/PGA multilayers, followed by assembly with Au DENPs formed using amine-terminated generation 5 (G5) poly (amidoamine) dendrimers as templates (Fig. 6). Similarly, Zhang *et al.*[56] prepared Fe_3O_4/polypyrrole (PPy)/Au core/shell NPs by coating PPy onto the preformed Fe_3O_4 NPs through the chemical oxidative polymerization of pyrrole and subsequent assembly of plentiful Au NPs on the surface of Fe_3O_4/PPy.

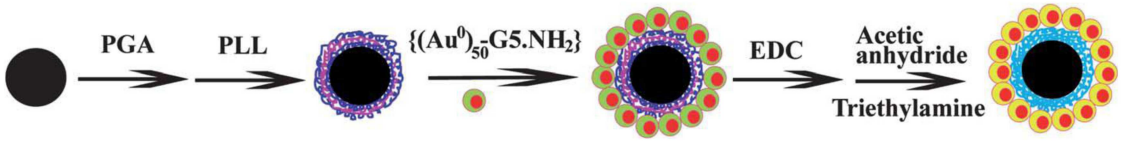


Fig. 6. Schematic representation of the fabrication of Fe_3O_4/Au CNPs.[6]

Although the polymer-mediated assembly approach is powerful to generate Fe_3O_4/Au CNPs, the approach usually involves multiple assembly steps and requires preformed Fe_3O_4 NPs and Au NPs. Recently, "one pot" hydrothermal route has been widely used to synthesize different NPs, such as Fe_3O_4 NPs, 3-aminopropyltrimethoxysilane (APTS)-coated Fe_3O_4 (Fe_3O_4/APTS) NPs,[57] and polyethyleneimine (PEI)-coated Fe_3O_4 (Fe_3O_4-PEI) NPs.[54] In a recent report, Li *et al.*[58] developed a "one pot" hydrothermal approach to synthesizing Fe_3O_4/Au CNPs with good water dispersibility and colloidal stability. In this work, PEI partially modified with poly(ethylene glycol) monomethyl ether (*m*PEG-PEI.NH_2) was used as a stabilizer to synthesize Au NPs via $NaBH_4$ reduction chemistry to form *m*PEG-PEI.NH_2-Au NPs. Then, those NPs were mixed with Fe (II) salt in a basic aqueous solution and autoclaved at elevated temperature and pressure. This process led to the formation of Fe_3O_4/Au CNPs with abundant PEI surface amines. After further acetylation of the PEI amines, the final Fe_3O_4/Au CNPs were formed. The *m*PEG modification and the final acetylation are intended to improve the biocompatibility of these CNPs for biomedical imaging applications.

3. Dual-mode MR/CT imaging applications of Fe_3O_4/Au CNPs

Fe_3O_4/Au CNPs have been used in a wide range of applications such as protein separation,[47] cell separation,[59] drug delivery and hyperthermia,[60–62] catalysis,[63] and biomedical imaging.[6,58,64] Herein, we will not introduce all of their applications; rather, we will discuss only their uses as contrast agents for dual-mode MR/CT imaging.

Although there are many reports related to the synthesis and characterization of the "dumbbell-like" Fe_3O_4/Au CNPs, only one report up to now attempted to use them for dual-mode MR and CT imaging.[1] By coating with amphiphilic poly(DMA-*r*-mPEGMA-*r*-MA) polymer, the particles were able to be imparted with water-dispersibility and antibiofouling properties. The Fe_3O_4/Au CNPs displayed a better X-ray attenuation property than pure Au NPs at the same Au concentration, which should be attributed to the presence of Fe_3O_4 NPs that also have an X-ray absorption property. Surprisingly, the T_2 relaxivity (r_2) of the Fe_3O_4/Au CNPs was measured to be 245 $mM^{-1}\cdot s^{-1}$, much higher than that of the commercial T_2 contrast agent (150 $mM^{-1}\cdot s^{-1}$). This increased r_2 is likely due to the synergistic effect when more than one Fe_3O_4 NP is linked to each Au NP, whereby the surrounding water molecules can be effectively influenced by the tiny multiple magnets in their vicinity. This synergistic effect in both X-ray attenuation and r_2 enabled this kind of "dumbbell-like" Fe_3O_4/Au CNPs to be used as an ideal dual-mode MR/CT imaging agent. Intravenous injection of the hybrid Fe_3O_4/Au CNPs into hepatoma-bearing mice resulted in high contrast between the hepatoma and normal hepatic parenchyma in both MR and CT imaging modes.

Different from the "dumbbell-like" Fe_3O_4/Au CNPs, the core/shell CNPs have been widely used as contrast agents for dual-mode MR and CT imaging applications. It is interesting to note that core/shell CNPs usually have a lower r_2 relaxivity when compared with Fe_3O_4 NPs because of the uniform

surface coating of Au. In an early work,[65] biocompatible core/shell Fe_3O_4/Au CNPs contrast agents were synthesized via green chemistry for MR and CT imaging. Both bare Fe_3O_4 and Fe_3O_4/Au CNPs were dispersed in agar gels with different Fe concentrations (0.06, 0.12, 0.24, 0.36, and 0.48 mM), with plain agar gel as the control. In the T_2-weighted MR phantom images, a noticeable darkening was observed with the Fe concentration for both bare Fe_3O_4 and Fe_3O_4/Au CNPs (Fig. 7(a)). Meanwhile, they showed similarly decreased MR signal intensity with the Fe concentration (Figs. 7(b) and 7(c)). It was further observed that the relaxation rate $(1/T_2)$ varied linearly with Fe concentration, and the r_2 relaxivity was measured to be 161 ± 2.48 $mM^{-1}\cdot s^{-1}$ for bare Fe_3O_4 particles and 124.2 ± 3.02 $mM^{-1}\cdot s^{-1}$ for Fe_3O_4/Au CNPs (Fig. 7(d)). The feasibility to use the Fe_3O_4/Au CNPs as CT contrast agents was also studied using a clinical CT scanner. To show their better imaging ability, Omnipaque (a popular iodine-based CT contrast agent currently in clinical use) was also compared. The results showed that the X-ray attenuation intensity of the Fe_3O_4/Au CNPs increased with increasing Au concentration, and was much higher than PBS, water, and bare Fe_3O_4 NPs even at the lowest Au concentration of 0.2 mg/mL (Fig. 8(a)). Figure 8(b) shows that the Fe_3O_4/Au CNPs with Au concentration of 4.4 mg/mL display an X-ray attenuation intensity similar to Omnipaque at the iodine concentration of 7.2 mg/mL. The results suggest that these Fe_3O_4/Au CNPs could be used as contrast agents for dual-mode MR and CT imaging applications.

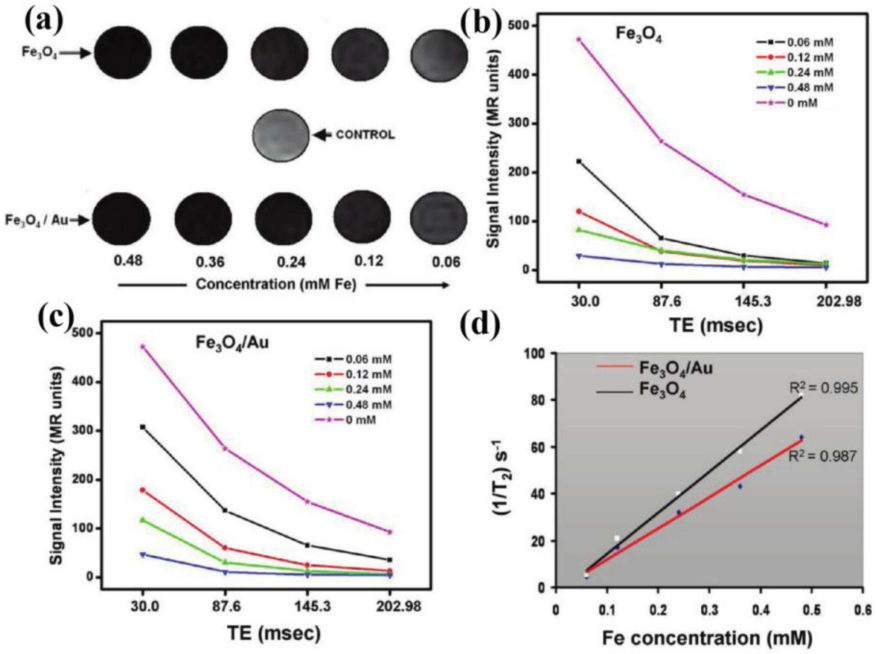


Fig. 7. MR imaging. (a) T_2-weighted MR phantom images of Fe_3O_4 and Fe_3O_4/Au CNPs with reference to control. (b), (c) Signal intensity versus TE plots for Fe_3O_4 and Fe_3O_4/Au CNPs, respectively. (d) T_2 relaxation rate $(1/T_2)$ versus Fe concentration.[65]

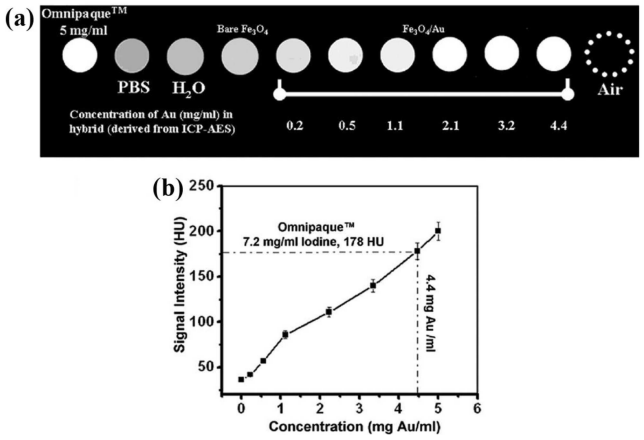


Fig. 8. CT imaging of CNPs. (a) CT images of the phantoms at 100 kVp with reference to control samples. (b) Au concentration (in CNPs) versus HU plot showing linear dependence.[65]

In a recent study, Fe_3O_4/Au CNPs prepared *via* LbL assembly of polymer multilayers and Au DENPs have also been used as contrast agents for dual-mode MR and CT imaging applications. In this work, the MR/CT imaging performance of different particles dispersed in an aqueous solution was evaluated. The results showed that Fe_3O_4/Au CNPs and Fe_3O_4/G5 NPs (Fe_3O_4/PGA/PLL/PGA/G5 NPs without Au NPs) also had a lower r_2 relaxivity when compared with the uncoated Fe_3O_4 NPs, which is due to the surface coating that limits the access of water molecules to the surface of Fe_3O_4 NPs.[23] For CT imaging, Fe_3O_4/Au CNPs, Fe_3O_4/G5 NPs, and Au DENPs were all able to induce CT contrast enhancement with the Au or Fe concentration. Further, Fe_3O_4/Au CNPs displayed much stronger X-ray attenuation intensity than Au DENPs at the same Au concentration and Fe_3O_4/G5 NPs at the same

Fe concentration, suggesting that the combination of both Au and Fe elements within one NP system can result in enhanced X-ray attenuation intensity for sensitive CT imaging applications. Their good MR and CT imaging performance enabled their uses as contrast agents for *in vivo* MR imaging of a mouse liver after intravenous injection and *in vivo* CT imaging of the right back of a mouse after subcutaneous injection (Fig. 9).

Another successful example to use core/shell Fe_3O_4/Au CNPs for MR/CT dual-mode imaging was reported by Li *et al.*[58] In their work, the "one pot" hydrothermally formed Fe_3O_4/Au CNPs were demonstrated to have a relatively high r_2 relaxivity (146.07 $mM^{-1}\cdot s^{-1}$, quite similar to the hydrothermally synthesized Fe_3O_4-PEI NPs without Au coating[54]) and a good X-ray attenuation property, which allowed them to be used for dual-mode MR/CT imaging applications. The non-compromised r_2 relaxivity may be due to the non-uniform coating of Au shell onto the Fe_3O_4 core. On one hand, the synthesized Fe_3O_4/Au CNPs were able to induce MR contrast enhancement of liver as a function of time post-injection after the particles were intravenously delivered to the mouse (Fig. 10). At 0.5 h post injection, the mouse liver showed a significantly reduced T_2 MR signal intensity compared to the initial one before injection. Subsequently, the signal intensity gradually recovered at 1 h post-injection due to the further metabolic process. On the other hand, the Fe_3O_4/Au CNPs were able to induce a clear CT contrast enhancement of the rat aorta (Fig. 11(a)) as indicated by the red arrow and the rat liver (as indicated by the white star) at 20 min post-injection. Quantitative CT value measurements show that the CT values of the liver and aorta are much higher than the initial respective values before injection (Fig. 11(b)). In addition, the CNPs did not display any visible hemolytic effect and apparent cytoxicity in the studied concentration range. Therefore, the formed CNPs may be used as a contrast agent for dual-mode MR/CT imaging applications *in vivo*.

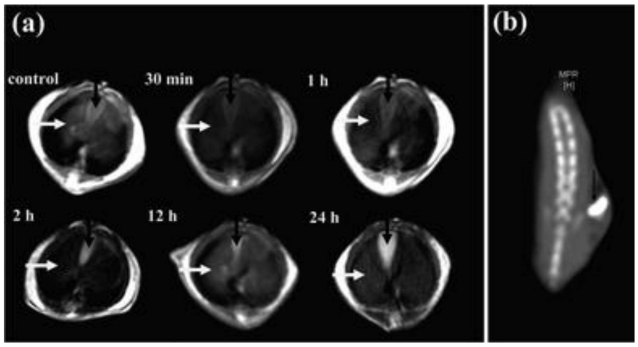


Fig. 9. (a) T_2-weighted MR images of mouse liver before and after intravenous injection of 0.1 mL Fe_3O_4/Au CNPs ([Fe] = 8.82 mg/mL, and [Au] = 1.57 mg/mL). In MR image, the black arrow indicates the gallbladder, while the white arrow indicates the liver. (b) CT image of a mouse subcutaneously injected with 0.5 mL Fe_3O_4/Au CNPs ([Fe] = 8.82 mg/mL, and [Au] = 1.57 mg/mL) into its back on the right at 5 min post-injection.[6]

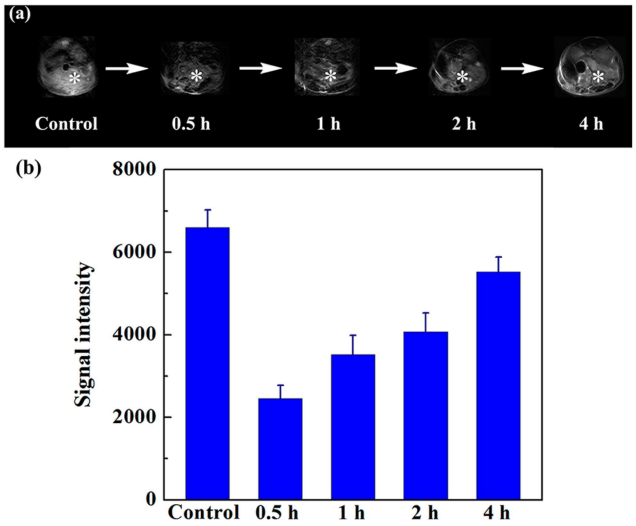


Fig. 10. T_2-weighted MR images (a) and signal intensity (b) of a mouse liver before injection and at different time points post intravenous injection of Fe_3O_4/Au CNPs (0.3 mL in PBS, [Fe] = 129.17 mM, [Au] = 68.46 mM).[58]

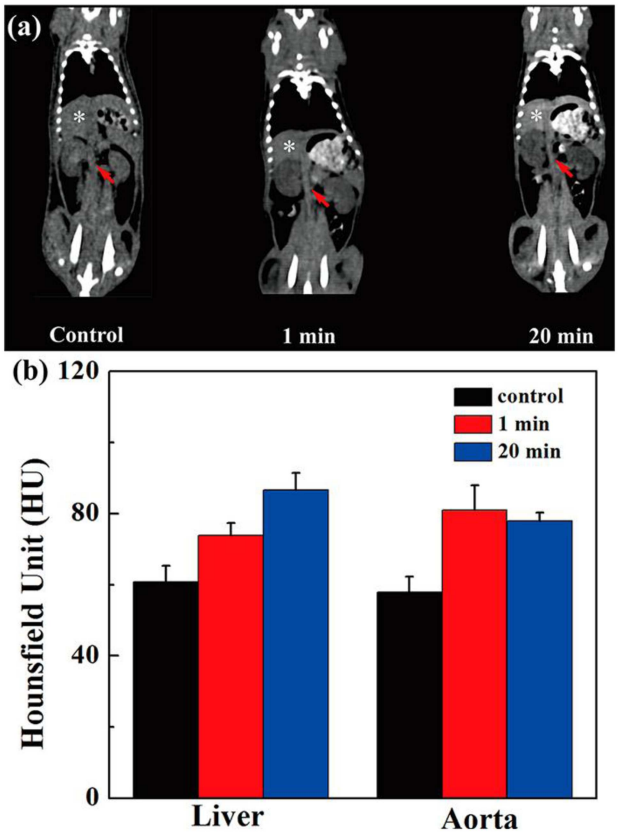


Fig. 11. CT images (a) and CT values (HU) (b) of rat liver and aorta before injection and at different time points post intravenous injection of Fe_3O_4/Au CNPs (1.0 mL in PBS, [Fe] = 129.17 mM, [Au] = 68.46 mM).[58]

In general, both "dumbbell-like" and "core/shell" Fe_3O_4/Au CNPs have more enhanced X-ray attenuation property than pure Au NPs due to the existence of Fe_3O_4 NPs. Unlike the "dumbbell-like" Fe_3O_4/Au CNPs, core/shell Fe_3O_4/Au CNPs always have lowered r_2 relaxivity when compared to uncoated Fe_3O_4 NPs due to the uniform coating of Au shells that limits the water accessibility to the surface of Fe_3O_4 NPs. To achieve a non-compromised r_2 relaxivity, one

strategy is to design non-uniform Au coating onto the surface of Fe_3O_4NPs.[58] The other strategy is to coat thin Au shells onto the surface of nanoclustered Fe_3O_4 NPs.[61] In a recent study, Ma *et al.*[61] reported a facile approach to forming thin gold shells onto the surface of the nanoclusters of 70 Fe_3O_4 NPs. The formed nanoclusters with a size of 30 nm possessed a higher r_2 relaxivity (219 $mM^{-1}\cdot s^{-1}$) than that of the "dumbbell-like" CNPs, which may be due to the porous structure of the nanoclusters and the thin gold coatings (3 nm) that result in short distances between Fe_3O_4 surfaces and water molecules, favoring high local inhomogeneities in the magnetic field.

4. Concluding remarks and outlooks

In summary, this review reports the recent advances in the synthesis or assembly of Fe_3O_4/Au CNPs for dual-mode MR/CT imaging applications. Fe_3O_4/Au CNPs with a "dumbbell-like" or "core/shell" type structure can be formed via controlled thermal deposition of iron precursor onto preformed Au NPs, direct coating of Au NPs onto preformed Fe_3O_4 NPs, seed-mediated growth methods, polymer-mediated assembly of Au NPs onto preformed Fe_3O_4 NPs, or hydrothermal formation of Fe_3O_4 NPs in the presence of preformed Au NPs. The Fe_3O_4/Au CNPs can be rendered with good biocompatibility after appropriate surface functionalization for dual-mode MR/CT imaging applications.

Although much effort has been devoted to the generation of Fe_3O_4/Au CNPs for MR/CT imaging applications, the preparation and development of these NP systems still remains an open area and offers great challenges. For instance, the formed "dumbbell-like" Fe_3O_4/Au CNPs have not been widely used for dual-mode MR/CT imaging applications so far. The versatility of nanotechnology may make it possible to synthesize other types of Fe_3O_4/Au CNPs via polymer-based approaches. With the rich macromolecular conjugation chemistry, the developed Fe_3O_4/Au CNPs can be further functionalized with targeting ligands, affording their uses as a targeted nanoprobe for dual-mode MR/CT imaging of tumors. Furthermore, it may be possible to conjugate anticancer drugs onto the surface of Fe_3O_4/Au CNPs for cancer theranostic applications.

References

[1] Kim D, Yu M K, Lee T S, Park J J, Jeong Y Y and Jon S 2011 *Nanotechnology* **22** 155101
[2] Yang H, Zhuang Y M, Sun Y, Dai A T, Shi X Y, Wu D M, Li F Y, Hu H and Yang S P 2011 *Biomaterials* **32** 4584
[3] Hu F Q and Zhao Y S 2012 *Nanoscale* **4** 6235
[4] Hu F Q, Jia Q J, Li Y L and Gao M Y 2011 *Nanotechnology* **22** 245604
[5] Niu D C, Luo X F, Li Y S, Liu X H, Wang X and Shi J L 2013 *ACS Appl. Mater. Interfaces* **5** 9942
[6] Cai H D, Li K G, Shen M W, Wen S H, Luo Y, Peng C, Zhang G X and Shi X Y 2012 *J. Mater. Chem.* **22** 15110
[7] Zhu J, Lu Y J, Li Y G, Jiang J, Cheng L, Liu Z, Guo L, Pan Y and Gu H W 2014 *Nanoscale* **6** 199
[8] Wang L J, Xing H Y, Zhang S J, Ren Q G, Pan L M, Zhang K, Bu W B, Zheng X P, Zhou L P and Peng W J 2013 *Biomaterials* **34** 3390
[9] Arvanitis C D, Livingstone M S and McDannold N 2013 *Phys. Med. Biol.* **58** 4749
[10] Xu B, Dou H, Tao K, Sun K, Ding J, Shi W B, Guo X S, Li J Y, Zhang D and Sun K 2011 *Langmuir* **27** 12134
[11] Patel D, Kell A, Simard B, Xiang B, Lin H Y and Tian G H 2011 *Biomaterials* **32** 1167
[12] Catana C, van der Kouwe A, Benner T, Michel C J, Hamm M, Fenchel M, Fischl B, Rosen B, Schmand M and Sorensen A G 2010 *J. Nucl. Med.* **51** 1431
[13] Schiepers C and Dahlbom M 2011 *Eur. Radiol.* **21** 548
[14] Xing H Y, Bu W B, Zhang S J, Zheng X P, Li M, Chen F, He Q J, Zhou L P, Peng W J and Hua Y Q 2012 *Biomaterials* **33** 1079
[15] Spernyak J A, White Iii W H, Ethirajan M, Patel N J, Goswami L, Chen Y, Turowski S, Missert J R, Batt C and Mazurchuk R 2010 *Bioconjugate Chem.* **21** 828
[16] Niedre M and Ntziachristos V 2008 *Proc. IEEE* **96** 382
[17] Melancon M P, Wang Y T, Wen X X, Bankson J A, Stephens L C, Jasser S, Gelovani J G, Myers J N and Li C 2007 *Invest. Radiol.* **42** 569
[18] Vuu K, Xie J W, McDonald M A, Bernardo M, Hunter F, Zhang Y T, Li K, Bednarski M and Guccione S 2005 *Bioconjugate Chem.* **16** 995
[19] Wu S C, Lin K L, Wang T P, Tzou S C, Singh G, Chen M H, Cheng T L, Chen C Y, Liu G C and Lee T W 2013 *Biomaterials* **34** 4118
[20] Cho H J, Yoon H Y, Koo H, Ko S H, Shim J S, Cho J H, Park J H, Kim K, Kwon I C and Kim D D 2012 *J. Control. Release* **162** 111
[21] Shi X Y, Thomas T P, Myc L A, Kotlyar A and Baker J R 2007 *Phys. Chem. Chem. Phys.* **9** 5712
[22] Wang S H, Shi X Y, Van Antwerp M, Cao Z Y, Swanson S D, Bi X D and Baker J R 2007 *Adv. Funct. Mater.* **17** 3043
[23] Shi X Y, Wang S H, Swanson S D, Ge S, Cao Z Y, Van Antwerp M E, Landmark K J and Baker J R 2008 *Adv. Mater.* **20** 1671
[24] Xu Z C, Hou Y L and Sun S H 2007 *J. Am. Chem. Soc.* **129** 8698
[25] Tian Q W, Hu J Q, Zhu Y H, Zou R J, Chen Z G, Yang S P, Li R W, Su Q Q, Han Y and Liu X G 2013 *J. Am. Chem. Soc.* **135** 8571
[26] Kobayashi Y, Inose H, Nagasu R, Nakagawa T, Kubota Y, Gonda K and Ohuchi N 2013 *Mater. Res. Innov.* **17** 507
[27] Gao L, Fei J B, Zhao J, Li H, Cui Y and Li J B 2012 *ACS Nano* **6** 8030
[28] Peng C, Zheng L F, Chen Q, Shen M W, Guo R, Wang H, Cao X Y, Zhang G X and Shi X Y 2012 *Biomaterials* **33** 1107
[29] Liu H, Wang H, Xu Y H, Shen M W, Zhao J L, Zhang G X and Shi X Y 2014 *Nanoscale* **6** 4521
[30] Hainfeld J F, Smilowitz H M, O'Connor M J, Dilmanian F A and Slatkin D N 2013 *Nanomedicine* **8** 1601
[31] Au J T, Craig G, Longo V, Zanzonico P, Mason M, Fong Y and Allen P J 2013 *Am. J. Roentgenol.* **200** 1347
[32] Kim D, Park S, Lee J H, Jeong Y Y and Jon S 2007 *J. Am. Chem. Soc.* **129** 7661
[33] Popovtzer R, Agrawal A, Kotov N A, Popovtzer A, Balter J, Carey T E and Kopelman R 2008 *Nano Lett.* **8** 4593
[34] Sun I C, Eun D K, Na J H, Lee S, Kim I J, Youn I C, Ko C Y, Kim H S, Lim D and Choi K 2009 *Chem. Eur. J.* **15** 13341
[35] Cui Y L, Wang Y N, Hui W L, Zhang Z F, Xin X F and Chen C 2005 *Biomed. Microdevices* **7** 153
[36] Chen C, Liu Y and Gu H Y 2010 *Microchim. Acta* **171** 371
[37] Wu W, He Q G, Chen H, Tang J X and Nie L B 2007 *Nanotechnology* **18** 145609
[38] Xu C J, Xie J, Ho D, Wang C, Kohler N, Walsh E G, Morgan J R, Chin Y E and Sun S H 2008 *Angew. Chem. Int. Ed.* **47** 173
[39] Xu C J, Wang B D and Sun S H 2009 *J. Am. Chem. Soc.* **131** 4216
[40] Yu H, Chen M, Rice P M, Wang S X, White R L and Sun S H 2005 *Nano Lett.* **5** 379
[41] Choi S H, Na H B, Park Y I, An K, Kwon S G, Jang Y, Park M H, Moon J, Son J S and Song I C 2008 *J. Am. Chem. Soc.* **130** 15573
[42] Kirui D K, Rey D A and Batt C A 2010 *Nanotechnology* **21** 105105
[43] Wood A, Giersig M and Mulvaney P 2001 *J. Phys. Chem. B* **105** 8810
[44] Haruta M 2004 *Gold Bull.* **37** 27
[45] El-Sayed I H, Huang X and El-Sayed M A 2005 *Nano Lett.* **5** 829
[46] Gupta A K, Naregalkar R R, Vaidya V D and Gupta M 2007 *Nanomedicine* **2** 23
[47] Bao J, Chen W, Liu T T, Zhu Y L, Jin P Y, Wang L Y, Liu J F, Wei Y G and Li Y D 2007 *ACS Nano* **1** 293
[48] Caruntu D, Cushing B L, Caruntu G and O'Connor C J 2005 *Chem. Mater.* **17** 3398
[49] Carril M, Fernández I, Rodríguez J, García I and Penadés S 2014 *Part. Part. Syst. Charact.* **31** 81

[50] Hu Y, Meng L, Niu L and Lu Q 2013 *ACS Appl. Mater. Interfaces* **5** 4586
[51] Bhana S, Rai B K, Mishra S R, Wang Y and Huang X 2012 *Nanoscale* **4** 4939
[52] Fan Z, Senapati D, Singh A K and Ray P C 2013 *Mol. Pharm.* **10** 857
[53] Guo R, Wang H, Peng C, Shen M W, Pan M J, Cao X Y, Zhang G X and Shi X Y 2010 *J. Phys. Chem. C* **114** 50
[54] Cai H D, An X, Cui J, Li J C, Wen S H, Li K G, Shen M W, Zheng L F, Zhang G X and Shi X Y 2013 *ACS Appl. Mater. Interfaces* **5** 1722
[55] Lu X Y, Niu M, Qiao R R and Gao M Y 2008 *J. Phys. Chem. B* **112** 14390
[56] Zhang H, Zhong X, Xu J J and Chen H Y 2008 *Langmuir* **24** 13748
[57] Shen M W, Cai H D, Wang X F, Cao X Y, Li K G, Wang S H, Guo R, Zheng L F, Zhang G X and Shi X Y 2012 *Nanotechnology* **23** 105601
[58] Li J C, Zheng L F, Cai H D, Sun W J, Shen M W, Zhang G X and Shi X Y 2013 *ACS Appl. Mater. Interfaces* **5** 10357
[59] Cui Y R, Hong C, Zhou Y L, Li Y, Gao X M and Zhang X X 2011 *Talanta* **85** 1246
[60] Son S J, Reichel J, He B, Schuchman M and Lee S B 2005 *J. Am. Chem. Soc.* **127** 7316
[61] Ma L L, Feldman M D, Tam J M, Paranjape A S, Cheruku K K, Larson T A, Tam J O, Ingram D R, Paramita V and Villard J W 2009 *ACS Nano* **3** 2686
[62] Ren J F, Shen S, Pang Z Q, Lu X H, Deng C H and Jiang X G 2011 *Chem. Commun.* **47** 11692
[63] Lin F H and Doong R A 2011 *J. Phys. Chem. C* **115** 6591
[64] Zhou T, Wu B Y and Xing D 2012 *J. Mater. Chem.* **22** 470
[65] Narayanan S, Sathy B N, Mony U, Koyakutty M, Nair S V and Menon D 2012 *ACS Appl. Mater. Interfaces* **4** 251